CHAPTER 3

On the Coupling of Viscous and Inviscid Models for Compressible Fluid Flows Via Domain Decomposition

R. Glowinski*
J. Periaux†
G. Terrasson**

Abstract. We discuss in this paper the coupling between the Navier-Stokes equations modelling compressible viscous flows with the time dependent full potential equation modelling compressible potential flows. The coupling is done through a domain decomposition procedure with overlapping; with such an approach one can take advantage of operator splitting techniques for the time discretization of the above equations.

Numerical results obtained from finite element approximations are presented showing that the present method provides a good quality matching technique.

1. Generalities. Synopsis.

The main goal of this paper is to present a computational method for the coupling of two distinct mathematical models describing the same physical phenomenon, namely the flow of a *compressible viscous fluid.* The basic idea is to replace the *Navier-Stokes equations* by the *potential* one in those regions where we can neglect the viscous effects and where the vorticity is small.

Consider for example a flow around an airfoil; we can split the computational domain into two overlapping subdomains:

—A first one, containing the airfoil, where the flow is modelled by the Navier-Stokes equations;

*Department of Mathematics University of Houston, Houston, TX 77204-3476 and Paris VI and INRIA, France.

†Avions Marcel Dassault, Saint-Cloud, France, and INRIA.

**Avions Marcel Dassault, Saint Cloud, France.

–A second, that we suppose to be sufficiently far from the airfoil so that the Navier-Stokes equations reduce there to the full potential equation for the velocity potential (assuming of course that in this second region, the flow is vorticity free).

Our goal here is to discuss a method for coupling both the *Navier-Stokes* and the *full potential* equations for *compressible fluids.* We will therefore describe the continuous equations, and then using a time discretization by operator splitting of the two sets of governing equations, reduce the original problem to a sequence of matching problems for linear models.

Then we will solve the matching problems by a GMRES type algorithm.

The possibilities of such techniques will be illustrated by the results of numerical experiments for 2-D flows around airfoils and/or inside air intakes.

2. Mathematical Modelings of the Flow Problems.

2.1. The compressible Navier-Stokes equations.

Let us consider the unsteady flow of a *compressible* viscous fluid around the body B (as shown on Figure 2.1, below):

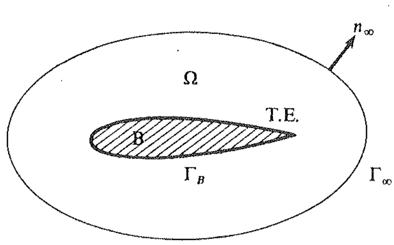

Figure 2.1

Flow around an airfoil B

We can use for the modelling of such flow the following (non conservative) system of partial differential equations:

(2.1) $$\frac{\partial \rho}{\partial t}+\nabla\cdot(\rho u) = 0 \ \textit{in}\ \Omega(=\mathbb{R}^N\backslash\bar{B}),$$

(2.2) $$\rho\,\frac{\partial u}{\partial t}+\rho(u\cdot\nabla)\, u+(\gamma-1)\,\nabla\rho T=\frac{1}{Re}\left[\nabla^2 u+\frac{1}{3}\,\nabla(\nabla\cdot u)\right]\ \textit{in}\ \Omega,$$

(2.3) $$\rho\frac{\partial T}{\partial t}+\rho u\cdot\nabla T+(\gamma-1)\rho\, T\,\nabla\cdot u=\frac{1}{Re}\left[\frac{\gamma}{Pr}\nabla^2 T+F(\nabla u)\right]\ \textit{in}\ \Omega,$$

where the pressure p, the density ρ and temperature T satisfy the *perfect gas law*

(2.4) $$p=(\gamma-1)\,\rho\, T\ (\textit{with}\ \gamma=1.4\ \textit{in air}).$$

In (2.1), (2.3), ρ, $u=\{u_i\}_{i=1}^N$ (N=2,3), T are the *non dimensionalized density, velocity* and *temperature*, respectively, with (if N=2)

(2.5) $$F(\nabla u)=\frac{4}{3}\left\{\left|\frac{\partial u_1}{\partial x_1}\right|^2+\left|\frac{\partial u_2}{\partial x_2}\right|^2-\frac{\partial u_1}{\partial x_1}\frac{\partial u_2}{\partial x_2}\right\}+\left|\frac{\partial u_1}{\partial x_2}+\frac{\partial u_2}{\partial x_1}\right|^2.$$

In the above equations Re, Pr and γ are the *Reynolds number*, the *Prandtl number*, and the *ratio of specific heats*, respectively.

From Γ_∞, we define

(2.6) $$\Gamma_\infty^- = \left\{x|x\in\Gamma_\infty,\ u_\infty\cdot n_\infty(x)<0\right\},\ \Gamma_\infty^+=\left\{x|x\in\Gamma_\infty,\ u_\infty\cdot n_\infty(x)\geq 0\right\},$$

($n_\infty(x)$=unit outward normal vector at Γ_∞, at x), and we prescribe on the *in flow boundary* Γ_∞^-

(2.7) $$u=u_\infty,\ \rho=1,\ T=1/\gamma(\gamma-1)M_\infty^2,$$

while on the *outflow boundary* Γ_∞^+, we prescribe Neumann and other "natural" boundary conditions.

On the wall Γ_B we shall use the following *Dirichlet boundary conditions*

(2.8) $$u=0,\ T=T_\infty\left(1+\frac{\gamma-1}{2}M_\infty^2\right).$$

In (2.7), (2.8), u_∞, T_∞, M_∞ denote the *free stream velocity, temperature* and Mach number, respectively. Finally, we shall also prescribe the following initial conditions

(2.9) $$\rho(x,\ 0)=\rho_o(x),\ u(x,\ 0)=u_o(x),\ T(x,\ 0)=T_o(x).$$

In order to render the above system of equations close to the incompressible flow model, we introduce the following new dependent variables

(2.10) $\sigma=\ln\rho$ (σ: *logarithmic density*).

With this new variable, the Navier-Stokes equations become

(2.11) $$\frac{\partial\sigma}{\partial t}+\nabla\cdot u+u\cdot\nabla\sigma=0,$$

(2.12) $$\frac{\partial u}{\partial t}+(u\cdot\nabla)u+(\gamma-1)(T\nabla\sigma+\nabla T)=\frac{e^{-\sigma}}{Re}\left(\nabla^2u+\tfrac{1}{3}\nabla(\nabla\cdot u)\right),$$

(2.13) $$\frac{\partial T}{\partial t}+u\cdot\nabla T+(\gamma-1)T\ \nabla\cdot u=\frac{e^{-\sigma}}{Re}\left(\frac{\gamma}{Pr}\nabla^2T+\ F(\nabla u)\right).$$

Equations (2.12), (2.13) can also be written as follows:

(2.14) $$\frac{\partial u}{\partial t}-\mu\nabla^2u+\beta\nabla\sigma=\Psi(\sigma,\ u,\ T),$$

(2.15) $$\frac{\partial T}{\partial t}-\Pi\nabla^2T=\chi(\sigma,\ u,\ T),$$

with:

(a) δ: a *mean value* of the *reciprocal of the density* ($\delta=1$ is a possible value),

(b) $$\nu=\frac{1}{Re},\ \mu=\nu\delta,\ \Pi\ =\ \frac{\gamma\nu\delta}{Pr},$$

(c) $$\beta=(\gamma-1)T_B=\frac{1}{\gamma}\left(\frac{\gamma-1}{2}+\frac{1}{M_\infty^2}\right),$$

(d) $$\Psi(\sigma, u, T)=-(\gamma-1)\,[\nabla T+(T-T_B)\nabla\sigma]-(u\cdot\nabla)u+\gamma e^{-\sigma}\left(\nabla^2 u+\frac{1}{3}\nabla(\nabla\cdot u)\right)-\nu\delta\Delta u,$$

(e) $$\chi(\sigma, u, T)=-(\gamma-1)T\nabla\cdot u-u\cdot\nabla T+\frac{\gamma\nu}{Pr}(e^{-\sigma}-\delta)\nabla^2 T+\nu e^{-\sigma}F(\nabla u).$$

2.2. The time dependent full potential equation.

If we suppose that viscosity and vorticity can be neglected, then the corresponding flow which is inviscid and potential is governed by the following full potential equations:

(2.16) $$\frac{\partial\rho}{\partial t}+\nabla\cdot\rho u=0,$$

(2.17) $$\rho=\rho_0\left(1-k(|\nabla\varphi|^2+2\frac{\partial\varphi}{\partial t})\right)^\alpha,$$

(2.18) $$T=T_\infty+\frac{1}{2\gamma}\left(1-|\nabla\varphi|^2-2\,\frac{\partial\varphi}{\partial t}\right).$$

In (2.17), (2.18), φ is the *velocity potential*; it satisfies

(2.19) $$u=\nabla\varphi.$$

In the above equations, ρ_0 is the flow density at rest, and

(2.20) $$T_\infty=\frac{1}{\gamma(\gamma-1)M_\infty^2},$$

(2.21) $$k=\frac{\gamma-1}{\gamma+1}\,\frac{1}{C_*^2},$$

(2.22) $$\alpha=\frac{1}{(\gamma-1)},$$

(2.23) γ: *ratio of specific heats,* (2.24) C_*: *critical velocity*, M_∞: *Mach number at infinity.*

For such a flow it is necessary to add boundary conditions such as

(2.25) $$\rho\frac{\partial\varphi}{\partial n}=0 \text{ on } \Gamma_B,$$

(2.26) $$u=u_\infty,\ \rho=\rho_o(1-k|u_\infty|^2)^\alpha=\rho_\infty \text{ at infinity.}$$

If we assume that the potential flow region contains Γ_∞, partly or entirely, we shall take as corresponding boundary condition

(2.27) $$\rho\frac{\partial\varphi}{\partial n}=\rho_\infty\, u_\infty\cdot n_\infty \text{ on } \Gamma_\infty,$$

where n_∞ denotes the unit outward normal vector at Γ_∞.

We decompose the computational domain (still denoted by Ω) into two subdomains, Ω_1 and Ω_2, such that the flow is governed by (2.1)-(2.4) in Ω_2, and by (2.16)-(2.19) in Ω_1. Notation is like in Figure 2.2, below:

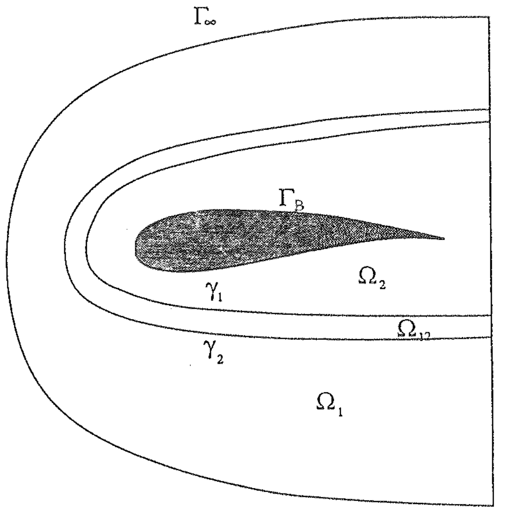

Figure 2.2

Decomposition of the computational domain

In Figure 2.2:

(a) $\Omega_{12}=\Omega_1 \cap \Omega_2$,

(b) γ_1 and γ_2 are the interfaces between Ω_{12} and Ω_2, Ω_{12} and Ω_1, respectively,

(c) $\Gamma_1=\Gamma_\infty \cap \partial\Omega_1$, $\Gamma_2=\Gamma_\infty \cap \partial\Omega_2$.

Our goal here is to solve (2.1)-(2.4) in Ω_2, coupled to (2.16)-(2.19) in Ω_1.

Actually, some extra boundary conditions have to be specified to obtain well-posed problems for $\{\sigma, \mathrm{u}, \mathrm{T}\}$ and φ; we shall take

(2.28) $\quad \varphi=\psi \text{ on } \gamma_1,$

(2.29) $\quad \mathrm{u}=\mathrm{v},\ \mathrm{T}=\tau \text{ on } \gamma_2.$

The problems associated to the trace of σ(or ρ) on γ_2 are more delicate and will be discussed later on; indeed the operator splitting approach will provide this information automatically. If the (yet unknown) traces ψ and $\{\mathrm{v}, \tau\}$ are specified, in (2.28), (2.29), then φ and $\{\sigma, \mathrm{u}, \mathrm{T}\}$ can be computed via equations (2.16)-(2.18) (on Ω_1) and (2.11)-(2.13) (on Ω_2), respectively.

In order to compute ψ and $\{\mathrm{v}, \tau\}$, and couple the two models, we can use a least squares approach in which we minimize over the overlapping region Ω_{12} some distance between u and $\nabla \varphi$, and, also, T and $\mathrm{T}(\varphi)$. This minimization problem takes the following form

$$(2.30)\qquad \begin{cases} \textit{Find } \bar{\psi} \textit{ and } \{\bar{\mathrm{v}}, \tau\} \textit{ such that} \\ \\ \mathrm{J}(\bar{\psi}, \bar{\mathrm{v}}, \bar{\tau}) \leq \mathrm{J}(\psi, \mathrm{v}, \tau), \quad \forall \{\psi, \mathrm{v}, \tau\}, \end{cases}$$

where in (2.30) we have (with A and B two positive weights):

$$(2.31)\qquad \mathrm{J}(\psi, \mathrm{v}, \tau)=\frac{1}{2}\int_{\Omega_{12}} |\mathrm{u}-\nabla\varphi|^2 d\mathrm{x} + \frac{\mathrm{A}}{2}\int_{\Omega_{12}} (\mathrm{T}-\mathrm{T}(\varphi))^2\, d\mathrm{x},$$

where $\{\mathrm{u}, \mathrm{T}\}$ (resp. $\{\bar{\mathrm{u}}, \bar{\mathrm{T}}\}$) is the solution in Ω_2 of the Navier-Stokes equations associated to $\{\mathrm{v}, \tau\}$ (resp. $\{\bar{\mathrm{v}}, \bar{\tau}\}$), with a similar definition for φ and $\bar{\varphi}$.

To solve this matching problem which is definitely *nonlinear*, we shall take advantage of a time discretization of the Navier-Stokes and full potential equations, based on operator splitting techniques; with such an approach, the time dependent coupling problem is reduced to a sequence of matching problems for linear time independent equations.

Remark 2.1: From a theoretical point of view, the above least squares formulation raises several questions, concerning, in particular the well posedness of the above problem, and more generally the choice of least squares criteria $J(\cdot)$ and functional spaces for which problem (2.30) makes sense. Indeed the above formulation makes sense for the finite element approximations of (2.30), (2.31).

Remark 2.2: Problem (2.30), (2.31) has the structure of an *optimal control problem* in the sense of J. L. Lions [1]; however unlike the *incompressible* case, previously discussed in [2], the solution of (2.30), (2.31) leads to quite complicated adjoint equations. Therefore, in practice, we shall systematically use *derivative free methods*, like those variants of the GMRES algorithm in which partial derivatives are approximated by *finite differences* (cf. [3]).

Remark 2.3: The minimization problem (2.30) is fairly complicated for the following reasons:

(i) The cost function (2.31) is non quadratic and the calculation of its derivative is rather complicated.

(ii) Formulation (2.30), (2.31) requires the adjustment of the weighting parameter A.

For the above reasons, we have chosen the following variant of the coupling problem:

We define first *residual functions* f_1, f_2, f_3, as follows:

$$(2.32)_1 \qquad <f_1, w_1>_1 = \int_{\Omega_{12}} (\nabla\varphi - u)\cdot\nabla w_1 dx, \ \forall\ w_1 \in V_1;\ f_1 \in V_1',$$

$$(2.32)_2 \qquad <f_2, w_2>_2 = \int_{\Omega_{12}} (u - \nabla\varphi)\cdot w_2\, dx, \ \forall w_2 \in V_2;\ f_2 \in V_2',$$

$$(2.32)_3 \qquad <f_3, w_3>_3 = \int_{\Omega_{12}} (T - T(\varphi))\, w_3 dx, \ \forall\ w_3 \in V_3,\ f_3 \in V_3'.$$

In the relations (2.32), the V_i are appropriate functional spaces with the V_i' as their dual spaces, and $<\cdot, \cdot>_i$ denotes the duality pairing between V_i' and V_i. The f_i's appear then as residuals associated to the coupling terms. Of course the ideal matching would be the one for which the above f_i's vanish simultaneously; in practice, we shall force them to be as small as possible, through a preconditioned GMRES algorithm to be described in Section 5.

3. Time discretization of the matching problem via operator splitting.

3.1. A time discretization of the compressible Navier-Stokes equations.

Following [4], we describe here a time discretization of the unsteady Navier-Stokes equations (2.1)-(2.4) in Ω_2, based on operator splitting methods.

Let $\Delta t>0$ be a time discretization step; with $\theta\in(0, \frac{1}{2})$, define a and b by

$$a=(1-2\theta)/(1-\theta), \quad b=\theta/(1-\theta). \tag{3.1}$$

Then, with obvious notation, we approximate the compressible Navier-Stokes equations on Ω_2 by (cf. [4]):

$$\sigma^o=\sigma_o=\ln\rho_o, \ u^o=u_o, \ T^o=T_o; \tag{3.2}$$

then for $n\geq 0$, *starting from* $\{\sigma^n, u^n, T^n\}$, *we solve*

$$\frac{\sigma^{n+\theta}-\sigma^n}{\theta\Delta t}+\nabla\cdot u^{n+\theta}=-u^n\cdot\nabla\sigma^n \ \textit{in} \ \Omega_2, \tag{3.3$_1$}$$

$$\frac{u^{n+\theta}-u^n}{\theta\Delta t}-a\mu\Delta u^{n+\theta}+\beta\nabla\sigma^{n+\theta}=\Psi(\sigma^n, u^n, T^n)+b\mu\Delta u^n \ \textit{in} \ \Omega_2, \tag{3.3$_2$}$$

$$\frac{T^{n+\theta}-T^n}{\theta\Delta t}-a\Pi\Delta T^{n+\theta}=\chi(\sigma^n, u^n, T^n)+b\Pi\Delta T^n \ \textit{in} \ \Omega_2, \tag{3.3$_3$}$$

$$\frac{\sigma^{n+1-\theta}-\sigma^{n+\theta}}{(1-2\theta)\,\Delta t}+u^{n+1-\theta}\cdot\nabla\sigma^{n+1-\theta}=-\nabla\cdot u^{n+\theta} \ \textit{in } \Omega_2, \tag{3.4$_1$}$$

$$\frac{u^{n+1-\theta}-u^{n+\theta}}{(1-2\theta)\Delta t}-b\mu\Delta u^{n+1-\theta}-\Psi\left(\sigma^{n+1-\theta},\, u^{n+1-\theta},\, T^{n+1-\theta}\right) \tag{3.4$_2$}$$

$$=a\mu\Delta u^{n+\theta}-\beta\nabla\sigma^{n+\theta} \ \textit{in } \Omega_2,$$

$$\frac{T^{n+1-\theta}-T^{n+\theta}}{(1-2\theta)\,\Delta t}-b\Pi\ \Delta T^{n+1-\theta}-\chi\left(\sigma^{n+1-\theta},\, u^{n+1-\theta},\, T^{n+1-\theta}\right) \tag{3.4$_3$}$$

$$=a\Pi\ \Delta T^{n+\theta} \ \textit{in } \Omega_2,$$

$$\frac{\sigma^{n+1}-\sigma^{n+1-\theta}}{\theta\Delta t}+\nabla\cdot u^{n+1}=-u^{n+1-\theta}\cdot\nabla\sigma^{n+1-\theta} \ \textit{in } \Omega_2, \tag{3.5$_1$}$$

$$\frac{u^{n+1}-u^{n+1-\theta}}{\theta\Delta t}-a\mu\Delta u^{n+1}+\beta\nabla\sigma^{n+1}=\Psi(\sigma^{n+1-\theta},\, u^{n+1-\theta},\, T^{n+1-\theta}) \tag{3.5$_2$}$$

$$+b\mu\Delta u^{n+1-\theta} \ \textit{in } \Omega_2,$$

$$\frac{T^{n+1}-T^{n+1-\theta}}{\theta\Delta t}-a\Pi\Delta T^{n+1}=\chi(\sigma^{n+1-\theta},u^{n+1-\theta},T^{n+1-\theta})+b\Pi\Delta T^{n+1-\theta} \ \textit{in } \Omega_2, \tag{3.5$_3$}$$

with $0<a,\ b<1,\ a+b=1$, satisfying (3.1). The boundary conditions will be specified later on.

3.2. Time discretization of the full potential equation.

We follow here the presentation in [5]. Let's consider first a *fully implicit* time discretization scheme of the equations (2.16)-(2.19). This scheme is of the *backward Euler* type and is defined as follows:

$$\varphi^0 \textit{ and } \rho^0 \textit{ are given in } \Omega_1; \tag{3.6}$$

then for $n\geq 0$, *assuming that* φ^n *and* ρ^n *are known, we obtain* φ^{n+1} *and* ρ^{n+1} *from the solution of*

$$\frac{\rho^{n+1}-\rho^{n}}{\Delta t}+\nabla\cdot(\rho^{n+1}\nabla\varphi^{n+1})=0 \text{ in } \Omega_1, \tag{3.7}$$

with in (3.7), ρ^{n+1} *given by*

$$\rho^{n+1}=\rho_o(1-k(|\nabla\varphi^{n+1}|^2+2\frac{\varphi^{n+1}-\varphi^{n}}{\Delta t}))^{\alpha}. \tag{3.8}$$

It follows from [6] that the above discretization is well suited to the numerical simulation of *lifting transonic flow, subsonic at infinity.* Indeed *operator splitting* ideas can also be applied here; our starting point is the fact that from—(2.17)—we have

$$\frac{\partial\rho}{\partial t}=(-2k\alpha)\rho_o\left(\frac{\rho}{\rho_o}\right)^{2-\gamma}\left(\nabla\varphi\cdot\nabla\frac{\partial\varphi}{\partial t}+\frac{\partial^2\varphi}{\partial t^2}\right). \tag{3.9}$$

Using (3.9), we can approximate (2.16)-(2.19) by the following θ-scheme, variant of (3.6)-(3.8):

Initialization:

$$\varphi^0 \text{ and } \rho^0 \text{ are given in } \Omega_1. \quad \square \tag{3.10}$$

Then for $n\geq 0$, *assuming that* φ^n *and* ρ^n *are known, we obtain* $\{\varphi^{n+\theta}, \rho^{n+\theta}\}$, $\{\varphi^{n+1-\theta}, \rho^{n+1-\theta}\}$, $\{\varphi^{n+1}, \rho^{n+1}\}$ *as follows:*

Step 1: *Solve, with respect to* $\varphi^{n+\theta}$, *the elliptic linear problem*

$$2k\alpha\rho_o\left(\frac{\rho^n}{\rho_o}\right)^{2-\gamma}\left(\nabla\varphi^n\cdot\nabla\left(\frac{\varphi^{n+\theta}-\varphi^n}{\theta\Delta t}\right)+\frac{\varphi^{n+\theta}+\varphi^{n-\theta}-2\varphi^n}{\theta^2|\Delta t|^2}\right)-\nabla\cdot\left(\rho^n\nabla\varphi^{n+\theta}\right)=0 \text{ in } \Omega_1, \tag{3.11}$$

then compute

$$\rho^{n+\theta}=\rho_o\left(1-k\left(|\nabla\varphi^{n+\theta}|^2+2\frac{\varphi^{n+\theta}-\varphi^n}{\theta\Delta t}\right)\right)^{\alpha}. \tag{3.12}$$

Step 2: *Solve, with respect to* $\varphi^{n+1-\theta}$, *the (nonlinear) problem*

$$\frac{\rho^{n+1-\theta}-\rho^{n+\theta}}{(1-2\theta)\Delta t}+\nabla\cdot\left(\rho^{n+1-\theta}\nabla\varphi^{n+1-\theta}\right)=0 \text{ in } \Omega_1, \tag{3.13}$$

where

$$\rho^{n+1-\theta}=\rho_o\left(1-k\left(|\nabla\varphi^{n+1-\theta}|^2+2\frac{\varphi^{n+1-\theta}-\varphi^{n+\theta}}{(1-2\theta)\Delta t}\right)\right)^{\alpha}. \tag{3.14}$$

<u>Step 3:</u> *Solve, with respect to* φ^{n+1}, *the elliptic linear problem.*

$$\begin{cases} 2k\alpha\rho_o\left(\frac{\rho^{n+\theta}}{\rho_o}\right)^{2-\gamma}\left(\nabla\varphi^{n+1-\theta}\cdot\nabla\left(\frac{\varphi^{n+1}-\varphi^{n+1-\theta}}{\theta\Delta t}\right)+\right. \\ \left. 2\frac{(1-2\theta)\varphi^{n+1}-(1-\theta)\varphi^{n+1-\theta}+\theta\varphi^{n+\theta}}{\theta(1-\theta)\ (1-2\theta)\ |\Delta t|^2}\right)-\nabla\cdot\left(\rho^{n+1-\theta}\nabla\varphi^{n+1}\right)=0 \text{ in } \Omega_1; \end{cases} \tag{3.15}$$

then compute

$$\rho^{n+1}=\rho_o\left(1-k\left(|\nabla\varphi^{n+1}|^2+2\frac{\varphi^{n+1}-\varphi^{n+1-\theta}}{\theta\Delta t}\right)\right)^{\alpha}. \tag{3.16}$$

3.3. <u>Time discretization for the coupling of the Compressible Navier-Stokes and Full Potential Equations.</u>

3.3.1 <u>Generalities.</u>

The fundamental idea behind the coupling strategy to be described below is to require the matching of the subdomain solutions (as defined in Section 2) only for the solutions of the linear subproblems encountered at the various steps of the operator splitting methods discussed in the above sections. Consequently, we shall "freeze" the interface conditions for the nonlinear subproblems, using at the interface boundary values predicted from the previous linear step. The implementation of these principles is described in the following sections.

3.3.2 Description of the matching method.

With Δt as above, we couple the θ-schemes (3.2)-(3.5) and (3.10)-(3.16), according to the matching criteria of Section 2.

Description of the algorithm: Using previous notation, we obtain

Step 0: Initialization.

$(3.17)_1$ $\quad \varphi^0$ *and* ρ^0 *are given in* Ω_1,

$(3.17)_2$ $\quad \sigma^0, u^0$ *and* T^0 *are given in* Ω_2. □

Then for $n \geq 0$, $\{\varphi^n, \rho^n\}$ *and* $\{\sigma^n, u^n, T^n\}$ *being known, we compute* $\{\varphi^{n+\theta}, \rho^{n+\theta}\}$, $\{\sigma^{n+\theta}, u^{n+\theta}, T^{n+\theta}\}$, *then* $\{\varphi^{n+1-\theta}, \rho^{n+1-\theta}\}$, $\{\sigma^{n+1-\theta}, u^{n+1-\theta}, T^{n+1-\theta}\}$, *and finally* $\{\varphi^{n+1}, \rho^{n+1}\}$, $\{\sigma^{n+1}, u^{n+1}, T^{n+1}\}$ *as follows:*

Step 1: *Solve the linear elliptic problem* (3.11) *with the boundary conditions*

(3.18) $\quad \rho^n \dfrac{\partial \varphi^{n+\theta}}{\partial n} = \rho_\infty\, u_\infty^{n+\theta} \cdot n$ *on* Γ_1, $\varphi^{n+\theta} = \psi^{n+\theta}$ *on* Γ_1, *to obtain* $\varphi^{n+\theta}$, *and use* (3.12) *to compute* $\rho^{n+\theta}$.

Solve now system (3.3) *with the boundary conditions*

(3.19) $\quad u^{n+\theta} = 0$ *on* Γ_B, $a\mu \dfrac{\partial u^{n+\theta}}{\partial n} - \beta\sigma^{n+\theta} n = -b\mu \dfrac{\partial u^n}{\partial n}$ *on* Γ_2, $u^{n+\theta} = v^{n+\theta}$ *on* γ_2,

(3.20) $\quad T^{n+\theta} = T_B$ *on* Γ_B, $\dfrac{\partial T^{n+\theta}}{\partial n} = 0$ *on* T_2, $T^{n+\theta} = \tau^{n+\theta}$ *on* γ_2.

In (3.18)-(3.20) *the traces* $\psi^{n+\theta}$, $v^{n+\theta}$, $\tau^{n+\theta}$ *are chosen such that*

(3.21) $$f_1^{n+\theta} = 0,\ f_2^{n+\theta} = 0,\ f_3^{n+\theta} = 0$$

(in a least squares sense at least).

Step 2: *Next, we look for* $\varphi^{n+1-\theta}$ and $\sigma^{n+1-\theta}$, $u^{n+1-\theta}$, $T^{n+1-\theta}$ *solutions of the nonlinear problems* (3.13) *and* (3.4), *for the following boundary conditions:*

(3.22) $$\rho^{n+1-\theta}\frac{\partial\varphi^{n+1-\theta}}{\partial n}=\rho_\infty u_\infty\cdot n \text{ on } \Gamma_1,\ \varphi^{n+1-\theta}=\psi^{n+\theta} \text{ on } \gamma_1,$$

(3.23) $$\sigma^{n+1-\theta}=\sigma^{n+\theta} \text{ on } \gamma_2\cup\Gamma_B,$$

(3.24) $$u^{n+1-\theta}=v^{n+\theta} \text{ on } \gamma_2,\ u^{n+1-\theta}=0 \text{ on } \Gamma_B,$$
$$b\mu\frac{\partial u^{n+1-\theta}}{\partial n}=\beta\sigma^{n+\theta}n-a\mu\frac{\partial u^{n+\theta}}{\partial n} \text{ on } \Gamma_2,$$

(3.25) $$T^{n+1-\theta}=\tau^{n+\theta} \text{ on } \gamma_2,\ T=T_B \text{ on } \Gamma_B,\ \frac{\partial T^{n+1-\theta}}{\partial n}=0 \text{ on } \Gamma_2.$$

Step 3: *Finally we compute* φ^{n+1} *and* σ^{n+1}, u^{n+1}, T^{n+1} *as the solutions of the linear systems* (3.15) *and* (3.5), *respectively, with* n *and* $n+\theta$ *replaced by* $n+1-\theta$ *and* $n+1$ *in the boundary conditions* (3.18) *and* (3.19), (3.20). □

Solution methods for solving the nonlinear problems in Step 2 are discussed in [5] and [7] (see also [8], [9] for the solution of the nonlinear potential flow problem); these methods are based on either least squares/conjugate gradient algorithms, or on GMRES type iterative methods (see [3]). In the following Section 4, we shall concentrate on the solution of the matching problems of Steps 1 and 3.

4. Solution of the matching problems.

4.1 Generalities.

In view of solving the matching problems associated to steps 1 and 3 of the algorithm described in Section 3.3.2 it is quite convenient to see them as *control problems* (cf., e. g., [1]) and to take as *control variables* the respective *traces* of the variables φ and $\{u, T\}$ on γ_1, γ_2, respectively (we drop the superscripts $n+\theta$ and $n+1$); we shall denote these traces by ψ and $\{v, \tau\}$. Once these traces have been specified, then φ and $\{u, T\}$ are *uniquely* defined as solutions of linear problems of the following type

$$(4.1)_1 \qquad a_o\varphi - \nabla\cdot(a_1\nabla\varphi) + A_2\cdot\nabla\varphi = f_1 \textit{ in } \Omega_1,$$

$$(4.1)_2 \qquad \varphi = \psi \textit{ on } \gamma_1,$$

$$(4.1)_3 \qquad a_1\frac{\partial\varphi}{\partial n} = g_1 \text{ on } \Gamma_1$$

(where a_o, a_1, A_2, f_1 and g_1 are known functions), and

$$(4.2)_1 \qquad \alpha\sigma + \nabla\cdot u = f_2 \textit{ in } \Omega_2,$$

$$(4.2)_2 \qquad \alpha u - a\mu\Delta u + \beta\nabla\sigma = g_2 \textit{ in } \Omega_2,$$

$$(4.2)_3 \qquad \alpha T - a\Pi\Delta T = h \textit{ in } \Omega_2,$$

$$(4.2)_4 \qquad \{u, T\} = \{v, \tau\} \textit{ on } \gamma_2,$$

$$(4.2)_5 \qquad u = 0,\ T = T_B \textit{ on } \partial B,$$

$$(4.2)_6 \qquad a\mu\,\frac{\partial u}{\partial n} - \beta\sigma n = k,\ T = T_\infty \textit{ on } \Gamma_2.$$

The above problems are discretized by the *finite element* methods discussed in [7], [5], [10], where a careful discussion of the compatibility between the spaces used for approximating u and σ is given.

The matching conditions taking place on the overlapping region Ω_{12} are achieved by

$$(4.3) \qquad \underset{\{\psi,\, v,\, \tau\}}{\text{Min}}\ j(\varphi, \sigma, u, T),$$

with φ, σ, u, T obtained from ψ, v, τ via the solution of the elliptic system (4.1), (4.2).

A possible candidate for j is given in Section 2 by (2.31); this minimization can be achieved by a conjugate gradient algorithm. Another alternative is based on the use of the GMRES algorithm and is defined as follows:

Considering the residuals associated to the matching problem *we force them to zero*, via a GMRES technique (described in Section 5). This GMRES algorithm is quite efficient in practice, but it has however some limitations that we would like to comment since they have practical implications. If the matching was perfect over Ω_{12} we should have

$$\int_{\Omega_{12}} (\nabla\varphi - \mathrm{u}) \cdot \nabla \mathrm{w} dx = 0, \forall \mathrm{w} \in H^1(\Omega_{12}), \tag{4.4}$$

$$\int_{\Omega_{12}} (\nabla\varphi - \mathrm{u})\cdot \mathrm{z} dx = 0, \forall \mathrm{z} \in \left(L^2(\Omega_{12})\right)^N, \tag{4.5}$$

$$\int_{\Omega_{12}} \Big(T - T(\varphi)\Big)\, \theta\, dx = 0, \forall\, \theta \in L^2(\Omega_{12}). \tag{4.6}$$

Satisfying (4.4) - (4.6) in a *least squares sense* by adjusting the "*control*" *variables* ψ, v and τ (defined over the interface γ_1 and γ_2) is always possible whatever Ω_{12} is; on the other hand solving (4.4) -(4.6) via GMRES seems to require that after an appropriate discretization, *the number of residual equations has to be equal to the dimension of the control space*; the limitations resulting from that contraint will appear clearly once we shall have defined the *finite element* spaces used to approximate φ, u, σ, T.

4.2 Finite Element Approximations

To approximate φ, u, σ, T we shall use the finite element spaces defined as follows:

1) Define a global triangulation $\mathcal{T}_h$ of the computational domain $\Omega_h = \Omega_{1h} \cup \Omega_{2h}$.

2) Define the triangulations $\mathcal{T}_{1h}$ and $\mathcal{T}_{2h}$ of Ω_{1h} and Ω_{2h} , respectively, in such a way that $\mathcal{T}_{1h}$ and $\mathcal{T}_{2h}$ coincide on $\Omega_{12h} = \Omega_{1h} \cap \Omega_{2h}$.

3) Starting from $\mathcal{T}_h$, we define $\mathcal{T}_{h/2}$ as the triangulation obtained from $\mathcal{T}_h$ by subdividing each triangle $K \in \mathcal{T}_h$ into 4 subtriangles, by joining the mid-points of each edge of K. Similarly we define $\mathcal{T}_{1h/2}$ and $\mathcal{T}_{2h/2}$.

4) The *potential* φ will be approximated on Ω_{1h} , using the finite element space V_{1h} defined by

$$V_{1h} = \left\{ w_h \,|\, w_h \in C^o(\bar{\Omega}_{1h}),\, w_h|_K \in P_1 ,\, \forall K \in \mathcal{T}_{1h/2} \right\}. \tag{4.7}$$

5) The *temperature* T and *logarithmic density* σ will be approximated on Ω_{2h} , using the space Q_{2h} defined by

(4.8) $$Q_{2h} = \left\{ q_h \mid q_h \in C^o(\bar{\Omega}_{2h}),\ q_h\,|_K \in P_1 ,\ \forall K \in \mathcal{T}_{2h} \right\}.$$

6) The *velocity* u will be approximated on Ω_{2h}, using the finite element space V_{2h} defined by

(4.9) $$V_{2h} = \left\{ z_h \mid z_h \in C^o(\bar{\Omega}_{2h}),\ z_h\,|_K \in P_1 \times P_1 ,\ \forall K \in \mathcal{T}_{2h/2} \right\}. \quad \square$$

In (4.7)-(4.9), P_1 denotes the space of the two variable polynomials of degree ≤ 1.

Using the above spaces, it is fairly easy to approximate the various boundary value problems providing φ_h, σ_h, u_h, T_h, respective approximations of φ, σ, u, T (see [5] for the details; see also [7] for the finite element approximation of the compressible Navier-Stokes equations, using spaces similar to Q_{2h} and V_{2h}).

Next we approximate (4.4) - (4.6) as follows: We introduce first the following subspaces W_{1h} . R_{2h}, W_{2h} of V_{1h}, Q_{2h}, V_{2h}, respectively (these spaces can be seen as the *control spaces* since they will contain the extensions over Ω_{12h} of the unknown traces ψ_h, v_h and τ_h). Actually W_{1h} (resp. R_{2h}, W_{2h}) are by definition generated by those basis functions of V_{1h} (resp. Q_{2h}, V_{2h}) associated to the vertices of $\mathcal{T}_{1h/2}$ (resp. $\mathcal{T}_{2h}$, $\mathcal{T}_{2h/2}$) belonging to γ_1 (resp. γ_2); these various notions have been visualized on Figure 4.1.

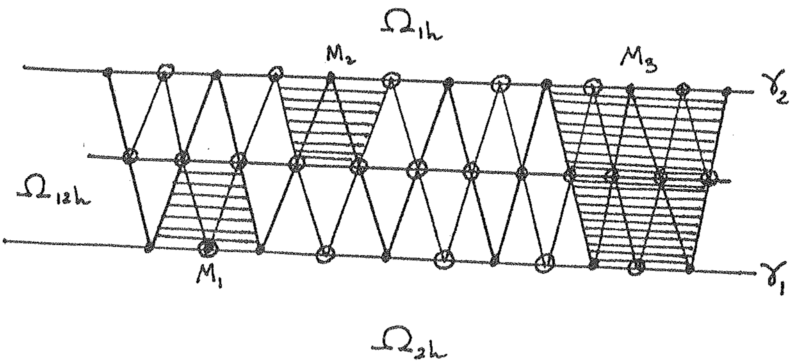

Figure 4.1: Detail of the overlapping region and of its triangulation.

We have indicated in particular the support of the basis function of W_{1h} (resp. R_{2h}, W_{2h})

associated to $M_1 \in \gamma_1$ (resp. M_2 , $M_3 \in \gamma_2$).

The discrete form of (4.4) - (4.6) is given by (we dropped the h in Ω_{12h}):

(4.10) $$\int_{\Omega 12}(\nabla\varphi_h - u_h) \cdot \nabla w_h \, dx = 0, \ \forall w_h \in W_{1h} ,$$

(4.11) $$\int_{\Omega 12}(\nabla\varphi_h - u_h) \cdot z_h \, dx = 0, \quad \forall z_h \in W_{2h} ,$$

(4.11) $$\int_{\Omega 12}\Big((T_h - T(\varphi_h)\Big) \cdot \theta_h \, dx = 0, \forall \theta_h \in R_{2h} .$$

We shall restrict the relations (4.10) - (4.11) to the basis functions of W_{1h} , W_{2h} , R_{2h} , respectively and therefore obtain a number of (nonlinear) equations which is equal to the dimension of the unknown trace vector $\{\psi_h , v_h , \tau_h \}$. In abstract form the matching problem can finally be written as

(4.13) $$F_h (\psi_h , v_h , \tau_h) = 0.$$

where F_h is obtained from the left hand sides of (4.10), (4.11), (4.12). The solution of (4.13) by a GMRES algorithm is adressed in the following Section 5.

5. On the GMRES solution of problem (4.13).

5.1. Generalities.

Instead of considering problem (4.13), directly, we shall consider first the GMRES solution of the following problem

(5.1) $$F(u) = 0,$$

where F is a (possibly nonlinear) operator from a *real Hilbert space* V into its dual space V'; we suppose that V is equipped with the scalar product $(\cdot,\cdot)$ and the corresponding norm $||\cdot||$. We denote by $<\cdot,\cdot>$ the *duality pairing* between V' and V, and by $S: V \to V'$ the associated *duality isomorphism*, i.e.

$$<Sv, w> = (v, w), \forall v, w \in V,$$

$$<Sv, w> = <Sw, v>, \forall v, w \in V,$$

$$<f, S^{-1} g> = (f, g)_*, \forall f, g \in V'.$$

5.2. Description of the GMRES algorithm for solving (5.1):

(5.2) $u^o \in V$ *is given;*

then for $n \geq 0$, u^n *being known we obtain* u^{n+1} *as follows:*

(5.3) $r_1^n = S^{-1} F(u^n)$,

(5.4) $w_1^n = r_1^n / \|r_1^n\|$;

Then for $j=2, \ldots k$, *compute* r_j^n *and* w_j^n *by*

(5.5) $r_j^n = S^{-1} DF(u^n; w_{j-1}^n) - \sum_{i=1}^{j-1} b_{ij-1}^n w_i^n$,

(5.6) $w_j^n = r_j^n / \|r_j^n\|$;

in (5.5), $DF(u^n; w)$ *is defined by either*

(5.7) $DF(u^n; w) = F'(u^n) \cdot w$

$\Big($*with* $F'(u^n)$ *the differential of* F *at* $u^n$$\Big)$ *or if the exact calculation of* F' *is too costly by*

(5.8) $DF(u^n ; w) = \dfrac{F(u^n + \varepsilon w) - F(u^n)}{\varepsilon}$,

with ε *sufficiently small. We define then*

(5.9) $$b^n_{il} = \langle DF(u^n\ ; w^n_l), w^n_i \rangle \left(=(S^{-1}\ DF(u^n\ ; w^n_l), w^n_i)\right).$$

Next, we solve the k-dimensional problem:

(5.10) $$\begin{cases} \textit{Find } a^n = \left\{a^n_j\right\}_{j=1}^{k} \in \mathbb{R}^k, \textit{ such that, } \forall b=\{b_j\}_{j=1}^{k} \in \mathbb{R}^k \textit{ we have} \\ \|F(u^n + \sum_{j=1}^{k} a^n_j\, w^n_j)\|_* \leq \|F(u^n + \sum_{j=1}^{k} b_j\, w^n_j)\|_*, \end{cases}$$

and we define u^{n+1} *by*

(5.11) $$u^{n+1} = u^n + \sum_{j=1}^{k} a^n_j\, w^n_j. \quad \square$$

Do $n = n+1$ *and go to* (5.3). $\square$

In algorithm (5.2)-(5.11), k is the dimension of the so-called *Krylov space.*

Remark 5.1: We should prove that

(5.12) $$(w^n_l, w^n_j) = 0,\ \forall\ 1 \leq l, j \leq k,\ j \neq l.$$

Remark 5.2: To compute $DF(u^n\ ; w)$, we can use instead of (5.8), the second order accurate discrete derivative

(5.13) $$DF(u^n\ ; w) = \frac{F(u^n + \varepsilon w) - F(u^n - \varepsilon w)}{2\varepsilon}.$$

Actually we are considering computing $DJ(u^n;w)$ within machine precision using the alternative differentiation procedures discussed in, e.g., [11] (see also the references therein).

Remark 5.3: In (5.10), the norm $\|\cdot\|_*$ satisfies the following relations

(5.14) $$\|f\|_* = \|S^{-1}\ f\ \| = \langle f, S^{-1}\ f\rangle^{1/2},\ \forall f \in V';$$

indeed we have used (5.14) to evaluate the various norms $\|\cdot\|_*$ occuring in (5.10).

Remark 5.4: In order to evaluate a^n via the solution of (5.11), it is sufficient to approximate in the neighborhood of b=0, the functional

$$(5.15)\qquad b \longrightarrow \|F\Big(u^n + \sum_{j=1}^{k} b_j w_j^n\Big)\|_*^2,$$

by the *quadratic* one defined by

$$(5.16)\qquad b \longrightarrow \|F\big(u^n\big) + \sum_{j=1}^{k} b_j \, DF(u^n\, ;\, w_j^n)\big)\|_*^2 .$$

Solving (5.16) is clearly equivalent so solving a linear system whose matrix k × k is symmetric and positive definite (this approach is equivalent to taking for a^n the first iterate provided by Newton's method applied to the solution of (5.15) and initialized with b=0).

5.3. Application to the solution of problem (4.13).

In this paragraph, we shall identify - for convenience - the trace functions ψ_h , v_h, τ_h with their, respective, (unique) extension over Ω_{12} belonging to W_{1h}, W_{2h}, R_{2h}. Therefore in the particular case of problem (4.13), the product space $W_{1h}\times W_{2h}\times R_{2h}=\mathcal{V}_h$ plays the role of the space V of sections 5.1, 5.2. As scalar product over v_h we have considered

$$(5.17)\ \Big(\big\{\psi_h^1,v_h^1,\tau_h^1\big\},\big\{\psi_h^2,v_h^2,\tau_h^2\big\}\Big)_{\mathcal{V}_h}=\int_{\Omega_{12}}\big(\nabla\psi_h^1\cdot\nabla\psi_h^2+v_h^1\cdot v_h^2+\tau_h^1\tau_h^2\big)dx,\ \forall\big\{\psi_h^i,v_h^i,\tau_h^i\big\}\in\mathcal{V}_h, i=1,2;$$

other choices are possible. Once (5.17) and the corresponding norm have been selected to provide $\mathcal{V}_h$ with an *Euclidian structure*, applying the GMRES algorithm of Section 5.2 is fairly easy; we have to observe, however, that

$$(5.18)\qquad \begin{cases} <F_h(\psi_h,\, v_h,\, \tau_h),\, \{w_h,\, z_h,\, \theta_h\}>_h = \\ \displaystyle\int_{\Omega_{12}} [(\nabla\varphi_h-u_h)\cdot\nabla w_h+(\nabla\varphi_h-u_h)\cdot z_h+(T_h-T(\varphi_h))\theta_h]dx, \\ \forall\{\psi_h,\, v_h,\, \tau_h\},\, \{w_h,\, z_h,\, \theta_h\}\in\mathcal{V}_h, \end{cases}$$

and to specify the analogue of S, i.e. the *preconditioning operator*. Concerning this last point we have experimented two operators S_h, the first one, S_{1h}, is associated to the scalar product (5.17), and in matrix form it will clearly have a block diagonal structure; the second operator, S_{2h}, is obtained by simply taking the (scalar) diagonal of S_{1h}, i.e.

(5.19) $$S_{2h} = \text{diag}\,(S_{1h}).$$

6. Numerical Experiments.

In this section we shall present the results of numerical experiments in which the methodology discussed in the above sections has been applied to the solution of two test problems. These two problems are namely

(i) A steady viscous flow around and inside a bi-NACA 0012 twin airfoil.

(ii) An unsteady viscous flow at high incidence around and inside an idealized two dimensional air intake.

6.1. Application to the bi-NACA 0012 twin airfoil.

We consider here an internal/external flow associated to the bi-NACA 0012 twin airfoil shown in Figures 6.1, 6.2. The angle of attack is 6 degrees, the Mach number at infinity is .55 and the Reynolds number based on the distance between the two airfoils is 200. Figure 6.1 shows the density triangulation employed to compute a global Navier-Stokes solution to be used as a reference (the velocity grid is twice finer); Figure 6.2 shows the subregion Ω_2 where the Navier-Stokes equations are used to model the flows together with the strip where the viscous and inviscid solutions are matched, located between γ_1 and γ_2. The steady solution has been obtained via a time dependent process using $\Delta t = .1$ for the θ-scheme and running 100 time cycles ($t = 10$). Figures 6.3 and 6.4 show the Mach contours for the global Navier-Stokes solution and the matched one, respectively; the agreement between these two calculations is quite good. Similarly, one has shown on Figure 6.5 (global solution) and Figure 6.6 (matched solution) the density contours; they agree quite well. On Figures 6.7-6.10 we have shown the skin friction coefficients (cf) and then the heat transfer coefficients (ch) for the upper and lower airfoils. Again the agreement between global and matched solutions is quite satisfactory.

On Figure 6.11 we have compared the efficiency of the matching algorithm, using the GMRES algorithm combined with the various preconditioners discussed in Section 5. The slowest algorithm corresponds to S_h =Identity, the intermediate to S_{1h} and the fastest to S_{2h} (block diagonal); using

S_{2h} leads to a speed up of two, measured in CPU, compared to the global solution calculation. Indeed further speed up can be obtained using parallel machines.

6.2. Application to an air intake.

For this test problem the geometry of the air intake is the one shown on Figures 6.12 and 6.13, where the corresponding density grids have also been visualized (for the global domain on Figure 6.12, for the Navier-Stokes domain Ω_2 in Figure 6.13). The above grid has been used to accurately simulate an unsteady flow at Re=200, M_∞=.6 for a 30 degrees angle of attack; for such data the flow is unsteady. We have used here Δt=.1, and Figures 6.14, 6.15 show the Mach contours of the reference global Navier-Stokes solution and of the matched one after 100 time cycles (t=10). Finally we compare on Figures 6.16, 6.17 the vorticity contours produced by the Navier-Stokes reference calculation, and the viscous/inviscid one.

Again we observe a very good agreement between the results obtained from both methods. More details, test cases and performance analysis can be found in [5].

7. Conclusion.

In the case of incompressible fluids, it was shown in [2] that domain decomposition provide robust and accurate methods for the coupling of mathematical models of a given physical phenomenon. From the results presented in this paper a similar conclusion can be drawn for the more complicated case addressed in this paper where conpressibility is taken into account.

Nevertheless, there is still room for many improvements such as efficient preconditioners, adaptive localization of the matching regions, efficient parallel implementations. It is our intention to extend these type of methods to the coupling of more complicated models, such as Euler and Navier Stokes equation or Boltzmann and Euler and/or Navier Stokes equations.

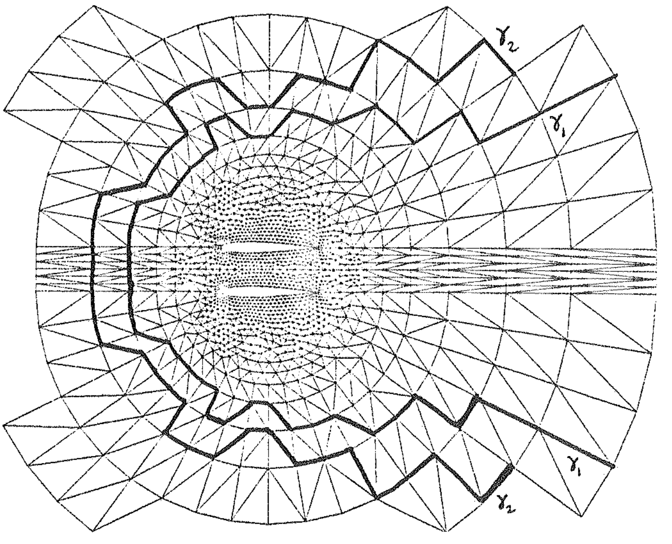

Figure 6.1: Bi-NACA 0012. Global Computational Domain

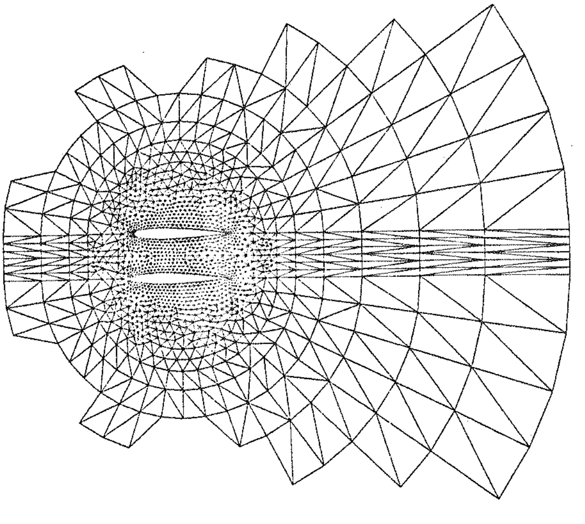

Figure 6.2: Bi-NACA 0012. Navier-Stokes Domain

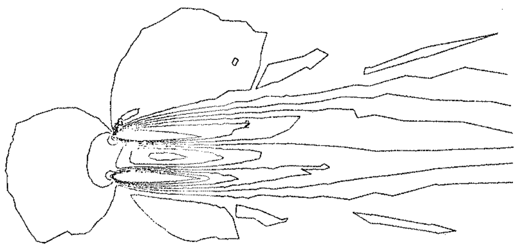

Figure 6.3: Bi-NACA 0012. Mach Contours of the Global Navier-Stokes Solution

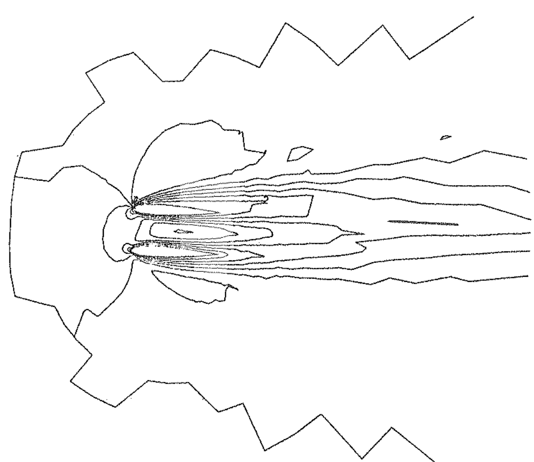

Figure 6.4: Bi-NACA 0012. Mach Contours of the matched solution.

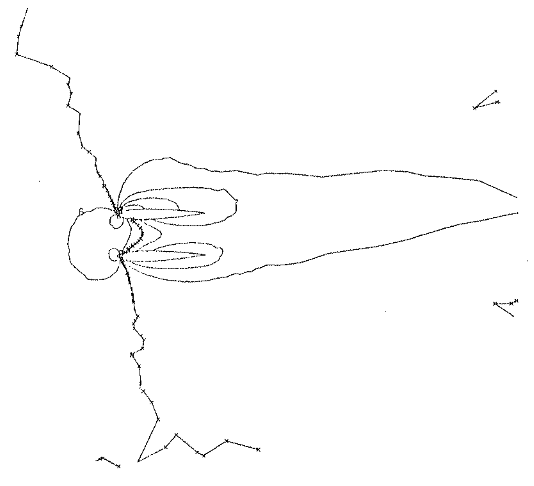

Figure 6.5: Bi-NACA 0012. Density Contours of the Global Navier-Stokes Solution

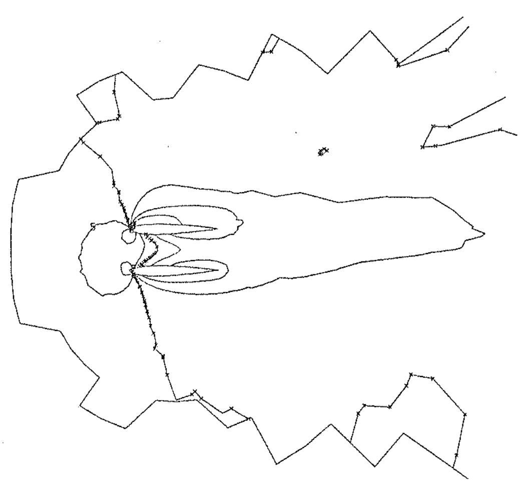

Figure 6.6: Bi-NACA 0012. Density Contours of the Matched Solution

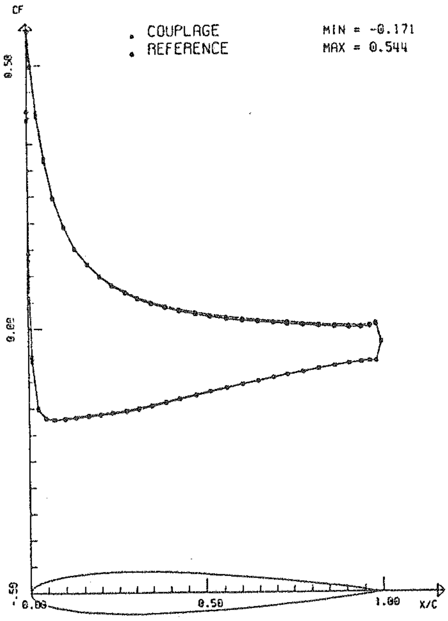

Figure 6.7: Bi-NACA 0012.
Skin Friction Coefficient
(Upper Airfoil)

Figure 6.8: Bi-NACA 0012
Skin Friction Coefficient
(Lower Airfoil)

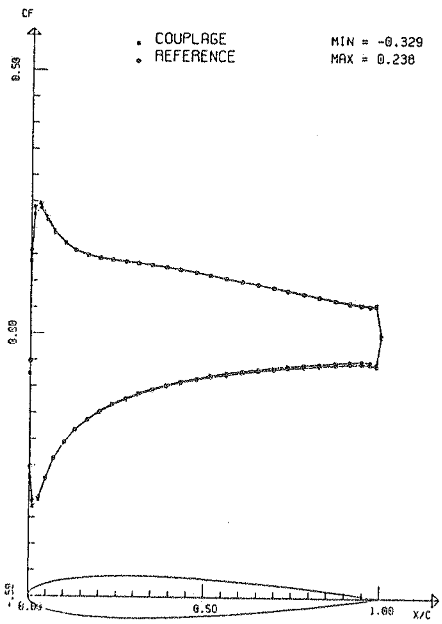

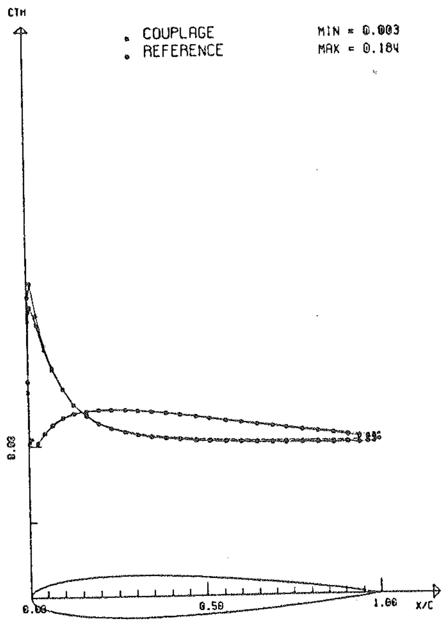

Figure 6.9: Bi-NACA 0012
Heat Transfer Coefficient
(Upper Airfoil)

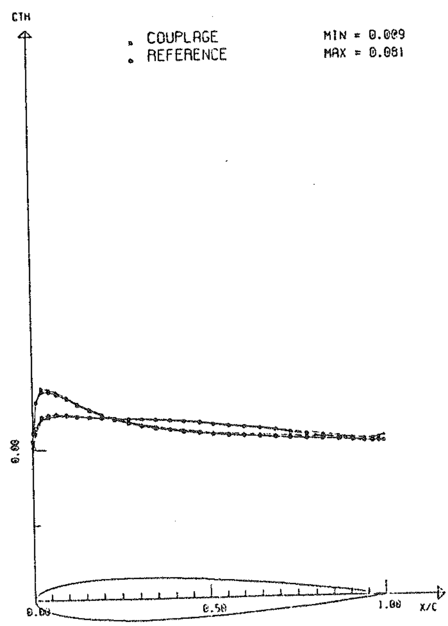

Figure 6.10: Bi-NACA 0012
Heat Transfer Coefficient
(Lower Airfoil)

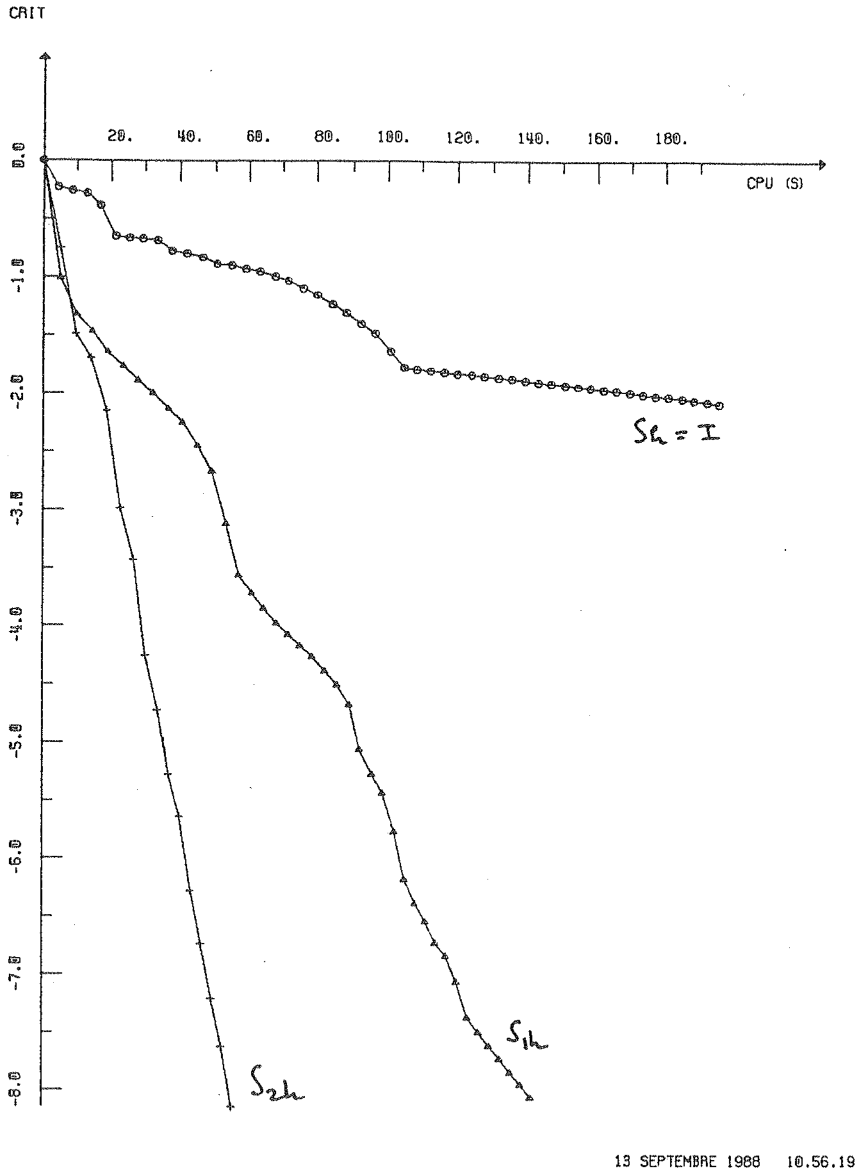

Figure 6.11: Bi-NACA 0012.
Convergence Behavior of the Matching
GMRES Algorithm.

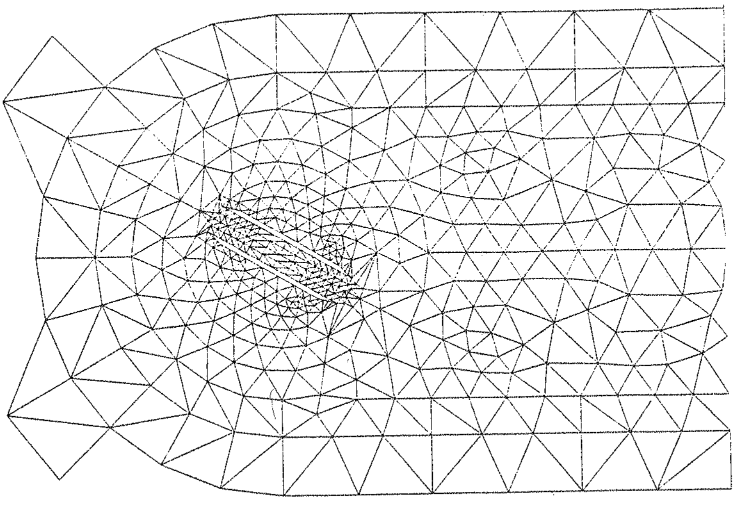

Figure 6.12: Two-Dimensional Nozzle
Global Computational Domain

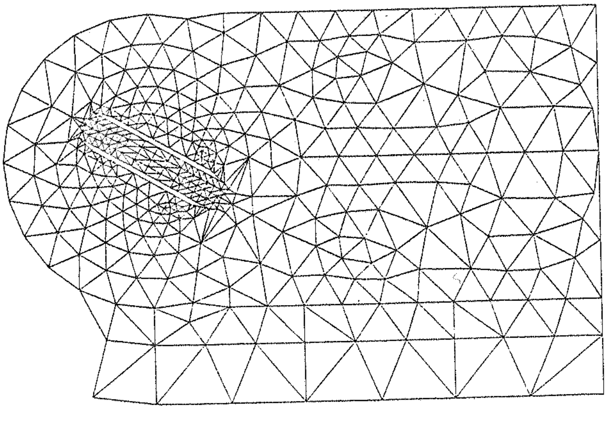

Figure 6.13: Two-Dimensional Nozzle.
Navier-Stokes Domain

Figure 6.14: Two-Dimensional Nozzle.
Mach Contours of the Global Navier-Stokes Solution.

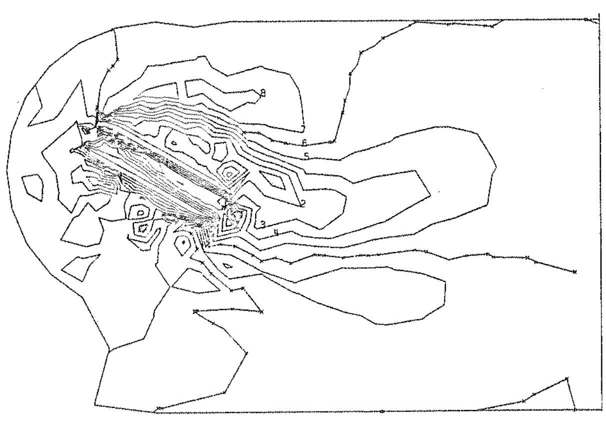

Figure 6.15: Two-Dimensional Nozzle.
Mach Contours of the Matched Solution.

Figure 6.16: Two-Dimensional Nozzle.
Vorticity Contours of the Global Navier-Stokes Solution

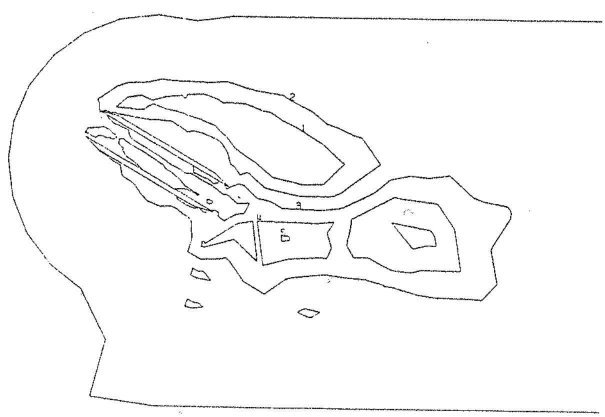

Figure 6.17: Two-Dimensional Nozzle.
Vorticity Contours of the Matched Solution.

Acknowledgment

The authors would like to thank Q. V. Dinh, M. O. Bristeau G. Roge, M. Storti and P. Le Tallec for helpful comments and suggestions. They also thank Lasonya Jones, Sherry Nassar, and Juana Wilson for the processing of this article and of a preliminary version of it. They acknowledge the support of Caltech and of the Fairchild Foundation, of DRET (Grant # 86-175), of the NSF (Grants DMS 8822522 and INT 8612680) and of LNCC-Rio de Janeiro.

References

[1] LIONS, J. L., *Controle Optimal des Systemes Gouvernes par des Equations aux Derivees Partielles*, Dunod, Paris, 1968.

[2] DINH, Q. V., GLOWINSKI, R., PERIAUX, J., TERRASSON, G., On the Coupling of Viscous and Inviscid Models for Incompressible Fluid Flows via Domain Decomposition, in *Domain Decomposition Methods for Partial Differential Equations*, R. Glowinski, G. H. Golub, G. Meurant, J. Periaux eds., SIAM, Philadelphia, pp. 350-369.

[3] BROWN, P. N., SAAD, Y., Krylov Methods for Nonlinear Systems of Equations, *Lawrence Livermore National Laboratory Research Report UCLR*-97649, Nov. 1987.

[4] BRISTEAU, M. O., GLOWINSKI, R., PERIAUX, J., Numerical Methods for the Navier-Stokes equations. Applications to the simulation of compressible and incompressible viscous flows, *Computer Physics Reports*, 6, (1987) pp. 73-187.

[5] TERRASSON, G., Simulation Numerique en Elements Finis d'Ecoulements de Fluides Visqueux Incompressibles et Compressibles par une Méthode de Couplage des Equations de Navier-Stokes et du Potentiel, *Thèse de Doctorat*, Université Pierre et Marie Curie, June 1989.

[6] STORTI, M., Numerical Simulation of Unsteady Potential Flows in Aerodynamics *Doctoral Thesis*, INTEC, Santa Fe, Argentina, 1990.

[7] BRISTEAU, M. O., GLOWINSKI, R., PERIAUX, J., Acceleration Procedures for the Numerical Simulation of Compressible and Incompressible Viscous Flows, in *Advances in Computational Nonlinear Mechanics*, J. S. Doltsinis ed., Springer-Verlag, Wien, 1989, pp. 197-243.

[8] GLOWINSKI, R., *Numerical Methods for Nonlinear Variational Problems*, Springer-Verlag, New York, 1984.

[9] BRISTEAU, M. O., GLOWINSKI, R., PERIAUX J., PERRIER P., PIRONNEAU, O., POIRIER, G., On the numerical solution of nonlinear problems in fluid dynamics by least squares and

finite element methods (II). Application to Transonic Flow simulation, *Comp. Meth. in Appl. Mech. Eng.*, 51, (1985), pp. 363-394.

[10] BRISTEAU, M. O., DUTTO, L., GLOWINSKI R., PERIAUX, J., ROGE, G., Compressible Viscous Flow Calculations using Compatible Finite Element Approximations, *Int. J. Num. Meth. Fluids* (to appear).